Arch Iran Med. March 2026;29(3):133-S1

doi:10.34172/aim.35172
http://journalaim.com

Supplementary Materials of

Patterns and Temporal Dynamics of Pediatric Solid Malignant Tumors: Insights from a 27-Year Referral Center Cohort in Iran (1996-2022)

For reader convenience, all supplementary tables, figures, and methods are fully hyperlinked.

Table of Contents

Supplementary Methods A. Age–Period–Cohort Analysis

In our Age–Period–Cohort analyses, we used generalized linear models (quasi-Poisson) with offset = log(population) to model referral-based incidence rates (population-standardized proxies). Sparse age × period × cohort cells were collapsed to improve model stability; however, even after collapsing, the model was parameterized using polynomial contrasts for age and period effects (linear, quadratic, cubic, etc.), and explicit contrasts for birth cohorts. Because case counts derive from a single tertiary referral center rather than a population-based registry, all modeled rates and effects represent referral-based diagnosis patterns rather than true population incidence.

As a result:

1. **Reference Categories**: The reference levels for the model remain age group 0–4 years, period 1996–1998, and birth cohort 1985. All estimates are relative to these reference categories.

2. **Polynomial Terms**: The reported coefficients (e.g., Age_Group.L, Age_Group.Q, Period.L, Period.Q, Period.C, Period^4–Period^8) correspond to linear, quadratic, cubic, and higher-order trend effects across the respective age or period groups.

3. **Rate Ratios**: Direct computation of individual group-level rate ratios (RRs) with 95% confidence intervals for each specific age, period, or cohort group is not possible from these polynomial-coded outputs. Instead, the coefficients describe the overall trends across categories.

Supplementary Methods B. Population Denominator Estimation

- Tehran Province Sensitivity Analysis: Population data were incomplete for several years, particularly 1996–2005 and 2017–2022. Missing values were estimated using:

1) Linear interpolation between the nearest observed SCI values for intermediate years.
2) One-sided gaps: For years beyond the last observed census, the last observed age- and sex-specific proportions were applied to known totals, or trends from the nearest complete census years (2006, 2011, 2016) were extrapolated.
3) Infant population (<1 year): Total births were split by sex using the stable sex ratio at birth (average 1.052–1.057 males/female across all years), and infant survival to year-end was applied.
4) Rounding: All population counts were rounded to the nearest whole number to match SCI reporting style.

This approach follows standard practices when official census data are unavailable for all years. These estimated denominators were used in sensitivity analyses restricted to Tehran Province.

These population denominators were used exclusively for rate standardization and sensitivity analyses and do not imply that resulting estimates represent population-level incidence.

Supplementary Table S1. **Annual Percent Change (APC) and Average Annual Percent Change (AAPC) of the total solid malignancies, Lymphomas, Central Nervous System (CNS) Tumors, and Sympathetic Nervous System (SNS) Tumors in the studied population (1996–2022)**

This table summarizes Joinpoint regression results for temporal trends in total pediatric solid malignancies and major tumor subtypes (lymphomas, CNS tumors, and SNS tumors) from 1996 to 2022. Segment-specific annual percent changes (APCs) with 95% confidence intervals (CIs) and p-values are reported for each identified joinpoint segment, along with overall average annual percent changes (AAPCs) for the full study period. Analyses are stratified by sex and age group where applicable. APCs and AAPCs were estimated based on referral-based rates of newly diagnosed cases, standardized using the national pediatric population as the denominator.

Table S1.

Malignancy			Annual Percent Change							Average Annual Percent Change			
		Segment	Start Segment	End Segment	Segment count	APC	95% Lower CI	95% Upper CI	P	AAPC	95% Lower CI	95% Upper CI	P
Total solid malignancies		0	1996	2009	634	4.4541	-12.3914	9.4704	0.283	6.0321	4.5872	7.6565	<0.001
		1	2009	2011	274	49.4638	1.5759	82.0238	0.049				
		2	2011	2022	1671	1.4856	-2.6017	5.6531	0.372				
Lymphomas	Total	0	1996	2022	428	3.5172	2.3519	5.0003	<0.001	3.5172	2.3519	5.0003	<0.001
	Male	0	1996	2022	303	2.7216	1.4144	4.3121	<0.001	2.7216	1.4144	4.3121	<0.001
	Female	0	1996	2022	125	4.6340	2.4032	8.3156	<0.001	4.6340	2.4032	8.3156	<0.001
	<1 y	0	1996	2014	6	0.5956*	-8.4146	5.8887	0.961	-3.4723	-8.0399	-0.1986	0.040
		1	2014	2016	8	119.446*	40.4368	377.2093	<0.001				
		2	2016	2022	6	-37.890*	-54.3692	-30.3497	<0.001				
	1-4 y	0	1996	2022	104	3.9414	1.8617	7.6148	0.004	3.9414	1.8617	7.6148	0.004
	0-4 y	0	1996	2022	124	4.6508	2.4870	8.1444	0.004	4.6508	2.4870	8.1444	0.004
	5-9 y	0	1996	2022	178	2.9458	1.0935	5.3196	0.004	2.9458	1.0935	5.3196	0.004
	10-14 y	0	1996	2022	126	3.2706	0.8395	6.0269	0.011	3.2706	0.8395	6.0269	0.011
CNS	Total	0	1996	2022	535	7.5611	5.8823	10.4732	<0.001	7.5611	5.8823	10.4732	<0.001
	Male	0	1996	2001	38	-14.212*	-56.1084	5.4089	0.206	4.7537	2.5638	8.3290	<0.001
		1	2001	2022	252	9.8557	7.6341	20.8442	0.023				
	Female	0	1996	2022	245	7.7619	5.7025	11.7702	<0.001	7.7619	5.7025	11.7702	<0.001
	<1 y	0	1996	2022	45	3.3300	0.3127	8.0113	0.033	3.3300	0.3127	8.0113	0.033
	1-4 y	0	1996	2022	209	6.5048	4.4774	10.693	<0.001	6.5048	4.4774	10.693	<0.001
	5-9 y	0	1996	2015	73	1.9882	-6.3085	5.7674	0.549	3.3419	0.4445	5.7468	0.035
		1	2015	2017	40	95.5931*	28.7887	233.9892	0.002				
		2	2017	2022	68	-19.396	-36.7353	-11.6809	0.002				
	10-14 y	0	1996	2007	33	-6.0851*	-42.1174	2.9114	0.181	6.1165	3.5071	9.7086	<0.001
		1	2007	2022	67	16.6205	11.2314	34.5412	0.002				
	5-14 y	0	1996	2012	89	-0.7548	-8.8383	3.3995	0.564	4.7299	2.3939	6.8765	<0.001
		1	2012	2017	83	42.3897	21.8469	98.5942	0.003				
		2	2017	2022	109	-8.5006	-27.9520	0.6505	0.068				
SNS	Total	0	1996	2022	518	8.4890	6.6870	11.7957	<0.001	8.4890	6.687	11.7957	<0.001
	Male	0	1996	2014	108	13.3537	10.1462	44.8041	0.002	8.7769	5.5179	15.1953	<0.001
		1	2014	2022	167	-1.4324*	-34.8233	6.8615	0.634				
	Female	0	1996	2022	243	8.3503	6.3035	12.3438	<0.001	8.3503	6.3035	12.3438	<0.001
	<1 y	0	1996	2022	94	5.3430	2.7796	10.0606	<0.001	5.3430	2.7796	10.0606	<0.001
	1-4 y	0	1996	2022	295	6.9812	5.1690	10.2659	<0.001	6.9812	5.1690	10.2659	<0.001
	5-9 y	0	1996	2022	106	8.2179	6.1189	13.0551	<0.001	8.2179	6.1189	13.0551	<0.001
	10-14 y	0	1996	2022	23	8.0729	5.5915	12.3375	<0.001	8.0729	5.5915	12.3375	<0.001

Abbreviation: AAPC, Average Annual Percent Change; APC, Annual Percent Change; CI, Confidence Interval, CNS, Central Nervous System; SNS, Sympathetic Nervous System; y, years.

* : Segments with low case counts yielded unstable APC estimates with wide confidence intervals and should be interpreted cautiously.

Supplementary Table S2. **Joinpoint Regression Model Diagnostics for Newly diagnosed Referral-Based Pediatric Solid Tumor Cases (1996–2022)**

This table presents diagnostic information for selected Joinpoint regression models corresponding to key tumor groups and selected age- and sex-specific subgroups. For each model, the number of joinpoints (#JP), permutation test p-values, segment-specific APCs with 95% CIs and statistical significance, and model fit statistics (sum of squared errors [SSE], mean squared error [MSE], degrees of freedom [DF], number of observations, and number of estimated parameters) are shown. These diagnostics support the validity and parsimony of the reported trend models.

All Joinpoint models evaluate temporal trends in referral-based population-standardized rates rather than true population incidence.

Table S2.

Cancer Group / Age / Sex	#JP	Permutation p-values	Segment-specific APCs (95% CI, significance)	SSE	MSE	DF	#Obs	#Param
All Solid Tumors	2	Test 0: 0.0047 Test 1: 0.0929 Test 2: 0.0238	Segment 0 (1996–2009): 4.45% (-12.39, 9.47, NS) Segment 1 (2009–2011): 49.46% (1.58, 82.02, S) Segment 2 (2011–2022): 1.49% (-2.60, 5.65, NS)	56.562	2.693	21	27	6
Lymphomas <1 years old	2	Test 0: 0.0031 Test 1: 0.0009 Test 2: 0.1162	Segment 0 (1996–2014): 0.60% (-8.41, 5.89, NS) Segment 1 (2014–2016): 119.45% (40.44, 377.21, S) Segment 2 (2016–2022): -37.89% (-54.37, -30.35, S)	6.444	0.307	21	27	6
CNS Males	1	Test 0: 0.0120 Test 1: 0.1578 Test 2: 0.1496	Segment 0 (1996–2001): -14.21% (-56.11, 5.41, NS) Segment 1 (2001–2022): 9.86% (7.63, 20.84, S)	26.288	1.143	23	27	4
CNS 5–9 years old	2	Test 0: 0.0129 Test 1: 0.0053 Test 2: 0.9529	Segment 0 (1996–2015): 1.99% (-6.31, 5.77, NS) Segment 1 (2015–2017): 95.59% (28.79, 233.99, S) Segment 2 (2017–2022): -19.40% (-36.73, -11.68, S)	18.464	0.879	21	27	6
CNS 10–14 years old	1	Test 0: 0.0269 Test 1: 0.0271 Test 2: 0.0138	Segment 0 (1996–2007): -6.09% (-42.12, 2.91, NS) Segment 1 (2007–2022): 16.62% (11.23, 34.54, S)	17.086	0.743	23	27	4
CNS 5–14 years old	2	Test 0: 0.0044 Test 1: 0.0180 Test 2: 0.4948	Segment 0 (1996–2012): -0.75% (-8.84, 3.34, NS) Segment 1 (2012–2017): 42.39% (21.85, 98.59, S) Segment 1 (2017–2022): -8.50% (-27.95, 0.65, NS)	24.006	1.143	21	27	6
SNS Males	1	Test 0: 0.0080 Test 1: 0.0382 Test 2: 0.1256	Segment 0 (1996–2014): 13.35% (10.15, 44.80, S) Segment 1 (2014–2022): -1.43% (-34.82, 6.86, NS)	29.365	1.277	23	27	4

Notes / Caption (Methods / Figure Legend):
Joinpoint regression analyses were conducted using the National Cancer Institute's Joinpoint Regression Program (version X.X.X). The optimal number of joinpoints for each group was selected using permutation tests (4499 permutations), with significance assessed at $\alpha = 0.05$. Segment-specific annual percent changes (APC) are reported with 95% confidence intervals; NS = not significant, S = significant. Goodness-of-fit metrics including residual sum of squares (SSE), mean squared error (MSE), degrees of freedom (DF), number of observations (#Obs), and number of model parameters (#Param) are provided. Residuals were uncorrelated for all models.

Abbreviations: CNS, Central Nervous System; DF, degrees of freedom; **#**JP, number of Jointpoints; MSE, mean squared error; NS, not significant; #Obs, number of observations; #Param, number of model parameters; S, significant; SNS, Sympathetic Nervous System; SSE, sum of squares.

Supplementary Table S3. **Age–Period–Cohort Model Estimates for Newly Diagnosed Referral-Based Lymphomas Cases (1996–2022) with Collapsed Sparse Categories.**

This table displays parameter estimates from age–period–cohort models assessing trends of newly diagnosed referral-based lymphomas cases from 1996 to 2022. To address sparse data, selected age, period, and birth-cohort categories were collapsed prior to modeling. Reported values include model coefficients, standard errors, test statistics, p-values, and 95% confidence intervals. Estimates are interpreted relative to the designated reference age group, period, and birth cohort.

All effects reflect referral-based diagnosis patterns and should not be interpreted as population-level incidence risks.

Table S3.

Age-Period-Cohort Model Term*	estimate	std.error	statistic	p.value	conf.low	conf.high
(Intercept)	0.000	0.095	-145.411	<0.001	0.000	0.000
Age_Group.L	0.864	0.069	-2.118	0.034	0.755	0.989
Age_Group.Q	0.944	0.046	-1.254	0.210	0.862	1.033
Period.L	3.729	0.138	9.549	<0.001	2.846	4.885
Period.Q	1.229	0.132	1.562	0.118	0.949	1.592
Period.C	0.989	0.127	-0.084	0.933	0.772	1.269
Period^4	1.249	0.125	1.777	0.076	0.977	1.596
Period^5	1.083	0.082	0.975	0.329	0.922	1.272
Period^6	1.872	0.116	5.402	<0.001	1.491	2.350
Period^7	1.710	0.090	5.990	<0.001	1.435	2.038
Period^8	1.772	0.121	4.720	<0.001	1.397	2.247
Birth_Cohort 1988-1990	0.801	0.122	-1.813	0.070	0.631	1.018
Birth_Cohort 1991-1993	1.477	0.130	3.002	0.003	1.145	1.905
Birth_Cohort 1994-1996	0.938	0.159	-0.401	0.689	0.687	1.281
Birth_Cohort 1997-1999	1.151	0.075	1.867	0.062	0.993	1.333
Birth_Cohort 2000-2002	0.519	0.145	-4.515	<0.001	0.390	0.690
Birth_Cohort 2003-2005	1.918	0.068	9.581	<0.001	1.679	2.191
Birth_Cohort 2006-2008	0.415	0.202	-4.353	<0.001	0.280	0.617
Birth_Cohort 2009-2011	0.886	0.104	-1.173	0.241	0.723	1.085
Birth_Cohort 2012-2014	0.405	0.255	-3.545	<0.001	0.246	0.668

*: Reference categories: age group '0-4', period group '1996–1998', and the earliest defined cohort '1985'.

Abbreviations: conf.high, higher 95% confidence interval; conf.low, lower 95% confidence interval; std.error, standard error.

Terms ending with .L, .Q, .C, or ^n represent **orthogonal polynomial contrasts** used in the Age–Period–Cohort model to capture trends across age and period groups:

- **Age_Group.L:** linear trend across age groups
- **Age_Group.Q:** quadratic trend across age groups
- **Period.L:** linear trend across period groups
- **Period.Q:** quadratic trend across period groups
- **Period.C:** cubic trend across period groups
- **Period^4:** fourth-order polynomial trend across period groups
- **Period^5:** fifth-order polynomial trend across period groups
- **Period^6:** sixth-order polynomial trend across period groups
- **Period^7:** seventh-order polynomial trend across period groups
- **Period^8:** eighth-order polynomial trend across period groups

These polynomial terms allow the model to capture nonlinear patterns in referral-based incidence across age and period while controlling for cohort effects. Estimates for these terms cannot be interpreted as simple group-level rate ratios (RRs); instead, their direction, magnitude, and statistical significance should be interpreted as representing the overall trend across the respective age or period variable.

Supplementary Table S4. **Age–Period–Cohort Model Estimates for Newly Diagnosed Referral-Based Central Nervous System (CNS) Tumor Cases (1996–2022) with Collapsed Sparse Categories.**

This table presents age–period–cohort model results for newly diagnosed referral-based CNS tumor cases over the study period (1996–2022) using collapsed sparse categories. Regression coefficients, standard errors, test statistics, p-values, and 95% confidence intervals are shown for age, period, and birth-cohort effects, with all estimates interpreted relative to their respective reference categories.

All effects reflect referral-based diagnosis patterns and should not be interpreted as population-level incidence risks.

Table S4.

Age-Period-Cohort Model Term*	estimate	std.error	statistic	p.value	conf.low	conf.high
(Intercept)	0.000	0.118	-124.841	<0.001	0.000	0.000
Age_Group.L	0.774	0.041	-6.186	<0.001	0.714	0.839
Age_Group.Q	1.580	0.057	8.023	<0.001	1.413	1.766
Period.L	1.862	0.154	4.049	<0.001	1.378	2.516
Period.Q	1.859	0.067	9.229	<0.001	1.630	2.121
Period.C	0.634	0.089	-5.138	<0.001	0.533	0.754
Period^4	0.563	0.160	-3.593	<0.001	0.411	0.770
Period^5	0.554	0.100	-5.913	<0.001	0.455	0.674
Period^6	0.493	0.174	-4.063	<0.001	0.350	0.693
Period^7	0.661	0.126	-3.287	0.001	0.517	0.846
Period^8	0.567	0.164	-3.459	0.001	0.411	0.782
Birth_Cohort 1988-1990	1.281	0.163	1.513	0.130	0.929	1.764
Birth_Cohort 1991-1993	1.113	0.175	0.610	0.542	0.790	1.568
Birth_Cohort 1994-1996	1.738	0.170	3.243	0.001	1.244	2.427
Birth_Cohort 1997-1999	0.923	0.103	-0.780	0.435	0.754	1.129
Birth_Cohort 2000-2002	2.219	0.182	4.391	0.000	1.555	3.167
Birth_Cohort 2003-2005	0.940	0.098	-0.633	0.527	0.775	1.139
Birth_Cohort 2006-2008	4.714	0.220	7.043	<0.001	3.062	7.258
Birth_Cohort 2009-2011	1.706	0.059	9.098	<0.001	1.521	1.915
Birth_Cohort 2012-2014	3.999	0.256	5.405	<0.001	2.419	6.611

*: Reference categories: age group '0-4', period group '1996–1998', and the earliest defined cohort '1985'.

Abbreviations: conf.high, higher 95% confidence interval; conf.low, lower 95% confidence interval; std.error, standard error.

Terms ending with .L, .Q, .C, or ^n represent **orthogonal polynomial contrasts** used in the Age–Period–Cohort model to capture trends across age and period groups:

- **Age_Group.L:** linear trend across age groups
- **Age_Group.Q:** quadratic trend across age groups
- **Period.L:** linear trend across period groups
- **Period.Q:** quadratic trend across period groups
- **Period.C:** cubic trend across period groups
- **Period^4:** fourth-order polynomial trend across period groups
- **Period^5:** fifth-order polynomial trend across period groups
- **Period^6:** sixth-order polynomial trend across period groups
- **Period^7:** seventh-order polynomial trend across period groups
- **Period^8:** eighth-order polynomial trend across period groups

These polynomial terms allow the model to capture nonlinear patterns in referral-based incidence across age and period while controlling for cohort effects. Estimates for these terms cannot be interpreted as simple group-level rate ratios (RRs); instead, their direction, magnitude, and statistical significance should be interpreted as representing the overall trend across the respective age or period variable.

Supplementary Table S5. **Age–Period–Cohort Model Estimates for Newly Diagnosed Referral-Based Sympathetic Nervous System (SNS) Tumor Cases (1996–2022) with Collapsed Sparse Categories.**

This table reports age–period–cohort model estimates for newly diagnosed referral-based SNS tumor cases from 1996 to 2022. Due to sparse observations in certain strata, selected categories were collapsed prior to analysis. The table includes estimated coefficients, standard errors, statistical tests, p-values, and 95% confidence intervals for age, period, and birth-cohort terms, relative to predefined reference groups.

All effects reflect referral-based diagnosis patterns and should not be interpreted as population-level incidence risks.

Table S5.

Age-Period-Cohort Model Term*	estimate	std.error	statistic	p.value	conf.low	conf.high
(Intercept)	0.000	0.514	-28.532	<0.001	0.000	0.000
Age_Group.L	0.389	0.168	-5.626	<0.001	0.280	0.540
Age_Group.Q	5.784	0.307	5.721	<0.001	3.170	10.552
Period.L	2.858	0.431	2.436	0.015	1.228	6.653
Period.Q	0.977	0.123	-0.192	0.848	0.767	1.243
Period.C	0.761	0.084	-3.251	0.001	0.646	0.897
Birth_Cohort1988-1990	0.653	0.338	-1.260	0.208	0.336	1.267
Birth_Cohort1991-1993	0.445	0.461	-1.758	0.079	0.180	1.098
Birth_Cohort1994-1996	0.840	0.516	-0.337	0.736	0.306	2.310
Birth_Cohort1997-1999	0.836	0.528	-0.339	0.734	0.297	2.353
Birth_Cohort2000-2002	1.311	0.529	0.512	0.609	0.465	3.697
Birth_Cohort2003-2005	1.511	0.627	0.658	0.511	0.442	5.167
Birth_Cohort2006-2008	1.644	0.574	0.866	0.387	0.533	5.070
Birth_Cohort2009-2011	1.028	0.814	0.034	0.973	0.208	5.067
Birth_Cohort2012-2014	1.413	0.813	0.425	0.670	0.287	6.958
Birth_Cohort2015-2017	0.911	1.030	-0.090	0.928	0.121	6.854

*: Reference categories: age group '0-4', period group '1996–1998', and the earliest defined cohort '1985'.

Abbreviations: conf.high, higher 95% confidence interval; conf.low, lower 95% confidence interval; std.error, standard error.

Terms ending with .L, .Q, .C, or ^n represent **orthogonal polynomial contrasts** used in the Age–Period–Cohort model to capture trends across age and period groups:

- **Age_Group.L:** linear trend across age groups
- **Age_Group.Q:** quadratic trend across age groups
- **Period.L:** linear trend across period groups
- **Period.Q:** quadratic trend across period groups
- **Period.C:** cubic trend across period groups

These polynomial terms allow the model to capture nonlinear patterns in referral-based incidence across age and period while controlling for cohort effects. Estimates for these terms cannot be interpreted as simple group-level rate ratios (RRs); instead, their direction, magnitude, and statistical significance should be interpreted as representing the overall trend across the respective age or period variable.

Supplementary Table S6. **Diagnostics and Goodness-of-Fit Statistics for Age–Period–Cohort Models Across Tumor Types.**

This table presents model diagnostics for APC analyses of referral-based Lymphomas, CNS, and SNS tumor diagnoses. For each tumor type, we report:

- Residual deviance and degrees of freedom (df residual) from quasi-Poisson models
- Estimated dispersion parameter
- AIC and BIC for Poisson and negative binomial (NB) models when applicable

These diagnostics provide information on model fit, overdispersion, and stability of individual parameter estimates, allowing for transparent interpretation of APC results. Values were used to inform choice of model (quasi-Poisson vs. NB) and to guide presentation of directional effects in the main text.

Diagnostics are reported to assess model stability for referral-based trend estimation rather than inference on absolute population incidence.

Table S6.

Statistic	Lymphomas	CNS	SNS
Residual deviance	70.14	214.61	202.54
df residual	24	24	24
Dispersion (Quasi-Poisson)	2.92	8.94	8.44
AIC (Poisson)	198.49	342.90	314.35
BIC (Poisson)	202.37	346.79	318.23
AIC (Negative Binomial)	181.10	209.31	189.85
BIC (Negative Binomial)	186.28	214.49	195.03

Abbreviations: AIC, Akaike Information Criterion; BIC, Bayesian Information Criterion; df, degree of freedom; CNS, Central Nervous System; SNS, Sympathetic Nervous System.

Supplementary Table S7. **Referral-Based Incidence Rate Ratios (IRRs) with 95% Confidence Intervals and Stratum Case Counts for Lymphomas, Central Nervous System (CNS), and Sympathetic Nervous System (SNS) Tumors by Age Group and Calendar Period.**

This table shows referral-based incidence rate ratios (IRRs) and 95% confidence intervals for lymphoma, CNS tumors, and SNS tumors across age groups (0–4, 5–9, and 10–14 years) and consecutive calendar periods. IRRs are estimated relative to the corresponding reference age group and period.

IRRs quantify relative changes in referral-based diagnosis rates across age groups and periods and should not be interpreted as estimates of population-level risk.

Table S7.

Age Group (years)	Period	Lymphomas				CNS				SNS			
		Stratum count*	IRR†	Lower 95%CI	Upper 95%CI	Stratum count*	IRR†	Lower 95%CI	Upper 95%CI	Stratum count*	IRR†	Lower 95%CI	Upper 95%CI
0-4	1996-2004	24	1	0.670	1.492	32	1	0.731	1.369	44	1	0.744	1.344
0-4	2005-2013	26	0.983	0.669	1.443	70	**1.674**	1.329	2.109	118	**2.432**	2.031	2.913
0-4	2014-2022	74	**2.410**	1.919	3.027	152	**3.107**	2.654	3.637	227	**4.033**	3.541	4.594
5-9	1996-2004	40	**1.436**	1.076	1.918	33	**0.692**	0.499	0.959	10‡	**0.170**	0.092	0.317
5-9	2005-2013	56	**2.223**	1.707	2.895	31	0.696	0.481	1.009	30	**0.661**	0.462	0.946
5-9	2014-2022	82	**2.777**	2.236	3.448	117	**2.438**	2.034	2.922	66	1.219	0.958	1.552
10-14	1996-2004	37	0.997	0.728	1.364	22	**0.330**	0.215	0.507	4‡	**0.056**	0.021	0.149
10-14	2005-2013	45	**1.578**	1.17	2.128	22	**0.316**	0.187	0.534	4‡	**0.080**	0.03	0.213
10-14	2014-2022	44	**1.671**	1.244	2.246	56	**1.332**	1.028	1.727	15	**0.311**	0.187	0.516

*: Raw case counts (N) for each stratum are reported here for transparency. The Haldane–Anscombe 0.5 correction was applied to these counts only for the calculation of descriptive incidence rates, but the raw integer counts (N) were used as the response variable in the regression models.

† : Incidence Rate Ratios (IRR) and 95% Confidence Intervals (CI) were derived from Generalized Linear Models (GLMs) incorporating log(PYAR) as an offset term. The modeling approach varied based on convergence stability: Lymphomas used Negative Binomial (NB) regression. CNS and SNS used standard Poisson regression due to persistent convergence failures in the NB model caused by extreme data sparsity, even after aggregation into 9-year periods. The reference category for all models is the 0–4 years old & 1996–2004 stratum (IRR = 1.000). Incidence Rate Ratios (IRRs) that demonstrate a statistically significant change (at the $p < 0.05$ level) compared to the reference group are highlighted in bold. Significance is determined by the 95% Confidence Interval excluding the null value of 1.000.

‡: For estimates based on $N \leq 10$ (i.e. high-uncertainty estimates).

Statistically significant IRR estimates are highlighted in **bold**.

Abbreviation: CI, Confidence Interval, CNS, Central Nervous System; IRR, Incidence Rate Ratios; SNS, Sympathetic Nervous System

Supplementary Table S8. **Annual Distribution and Scope of Referral Provinces for Pediatric Solid Malignant Tumors (1996–2022).**

This table addresses the stability of the center's referral catchment by detailing the geographic origin of cases over the study period. It shows the number and percentage of solid tumor cases referred annually from Tehran Province (the center's location) versus all other provinces. The table also provides the total number and proportion of Iran's provinces represented in the cohort each year. The data consistently show that a majority of cases were referred from outside Tehran (ranging from 57.6% to 67.0%), indicating a stable, broad national referral scope over the 27 years.

Table S8.

	N / %	1996	1997	1998	1999	2000	2001	2002	2003	2004
Tehran province	N	18	13	14	11	13	11	14	13	10
	%	31.0	33.3	27.5	28.2	28.3	33.3	29.2	25.5	27.0
Non-Tehran provinces	N	35	23	33	25	29	19	30	34	24
	%	60.3	59.0	64.7	64.1	63.0	57.6	62.5	66.7	64.9
Unknown	N	5	3	4	3	4	3	4	4	3
	%	8.6	7.7	7.8	7.7	8.7	9.1	8.3	7.8	8.1
No. of provinces represented*	N / total (%)	25/26 (96.2)	27/27 (100.0)	27/28 (96.4)	26/28 (92.9)	28/28 (100.0)	28/28 (100.0)	27/28 (96.4)	28/28 (100.0)	26/28 (92.9)
	N / %	**2005**	**2006**	**2007**	**2008**	**2009**	**2010**	**2011**	**2012**	**2013**
Tehran province	N	16	18	17	14	17	30	40	29	41
	%	27.1	31.6	25.8	28.0	31.5	31.3	32.3	25.7	31.5
Non-Tehran provinces	N	38	34	44	32	32	58	73	74	78
	%	64.4	59.6	66.7	64.0	59.3	60.4	58.9	65.5	60.0
Unknown	N	5	5	5	4	5	8	11	10	11
	%	8.5	8.8	7.6	8.0	9.3	8.3	8.9	8.8	8.5
No. of provinces represented*	N / total (%)	28/30 (93.3)	28/30 (93.3)	27/30 (90.0)	27/30 (90.0)	28/30 (93.3)	29/30 (96.7)	30/31 (96.8)	29/31 (93.5)	29/31 (93.5)
	N / %	**2014**	**2015**	**2016**	**2017**	**2018**	**2019**	**2020**	**2021**	**2022**
Tehran province	N	47	42	37	55	63	32	61	54	47
	%	30.3	27.1	28.2	29.9	33.3	28.6	35.5	31.8	29.4
Non-Tehran provinces	N	95	103	85	119	116	75	101	107	106
	%	61.3	66.5	64.9	64.7	61.4	67.0	58.7	62.9	66.3
Unknown	N	13	10	9	10	10	5	10	9	7
	%	8.4	6.5	6.9	5.4	5.3	4.5	5.8	5.3	4.4
No. of provinces represented*	N / total (%)	31/31 (100.0)	28/31 (90.3)	27/31 (87.1)	28/31 (90.3)	28/31 (90.3)	28/31 (90.3)	26/31 (83.9)	26/31 (83.9)	28/31 (90.3)

* : number of provinces has changed multiple times in Iran since 1996

Supplementary Table S9. **Sensitivity Analysis of Temporal Trends in Pediatric Solid Malignancies Using Tehran Province Pediatric Population as the Denominator (Joinpoint Regression, 1996–2022).**

This table presents the results of a sensitivity analysis assessing temporal trends in pediatric solid malignancies and major tumor subtypes using the pediatric population of Tehran Province as the denominator. This analysis was conducted to evaluate the robustness of the study findings to uncertainty in the true referral catchment population of the study center, which functions as a national referral hospital rather than a population-based cancer registry.

For each malignancy, Joinpoint regression models were fitted to identify statistically significant changes in temporal trends over the study period (1996–2022). The table reports segment-specific annual percent changes (APCs) with corresponding 95% confidence intervals (CIs), along with p-values derived from the Monte Carlo permutation tests used by the Joinpoint Regression Program to select the optimal number of joinpoints. Model diagnostics, including sum of squared errors (SSE), mean squared error (MSE), degrees of freedom (DF), number of observations (#Obs), and number of estimated parameters (#Param), are provided for the selected models.

The results shown in this table are based exclusively on Tehran Province population denominators and are intended as a robustness check. The primary Joinpoint analyses using the national pediatric population as the denominator are presented separately in Supplementary Table 1. The overall consistency in the direction and significance of temporal trends between the Tehran-only and national analyses supports the internal validity of the study and reinforces that the manuscript's conclusions are appropriately focused on temporal patterns rather than absolute population incidence rates.

As with the primary analyses, these estimates represent referral-based population-standardized trends rather than true population incidence.

Table S9.

Malignancy	Annual Percent Change								Model Diagnostics					
	Segment	Start Segment	End Segment	Segment count	APC	95% Lower CI	95% Upper CI	P	**Permutation p-values**	SSE	MSE	DF	#Obs	#Param
Total solid malignancies	1	1996	2008	168	−1.832	−14.321	2.613	0.3299	0.0089	26.85	1.278	21	27	6
	2	2008	2011	101	44.351	13.092	63.373	0.0044	0.0224					
	3	2011	2022	508	2.234	−2.634	5.110	0.2751	0.0104					
Lymphomas	1	1996	2003	29	−7.210	−29.030	1.241	0.1084	0.0018	4.49	0.195	23	27	4
	2	2003	2022	101	4.522	2.694	11.391	0.020	0.0229					
CNS	1	1996	2001	20	−23.322	−58.832	−1.214	0.0356	0.0007	22.03	0.958	23	27	4
	2	2001	2022	142	11.021	8.752	16.782	0.002	0.0327					
SNS	1	1996	2022	153	8.260	6.372	11.792	<0.001	0.4009	21.27	0.851	25	27	2

Joinpoints were selected using Monte Carlo permutation tests (4,499 permutations) with an overall significance level of 0.05. Models were fit using log-linear regression with Poisson variance. SSE, MSE, degrees of freedom, number of observations, and model parameters are reported for the selected final model. Residuals were uncorrelated for all models.

Abbreviations: DF, degrees of freedom; **#**JP, number of Jointpoints; MSE, mean squared error; NS, not significant; #Obs, number of observations; #Param, number of model parameters; S, significant; SSE, sum of squares.

* : Indicates estimates with wide confidence intervals, reflecting sparse data within the corresponding stratum; results should be interpreted with caution.

Supplementary Figure S1. **Temporal trends of pediatric oncology and solid tumor load as a proportion of non-oncology pediatric elective surgeries (1996–2022).**

To address concerns regarding potential changes in hospital capacity, referral intensity, or preferential referral pathways over time, we conducted an internal assessment using non-oncology pediatric elective surgeries as a stable institutional benchmark. Because elective surgical volume is largely independent of oncology referral patterns, it provides a pragmatic proxy for the center's overall clinical capacity and operational stability across years. This assessment is presented in Supplementary Figure X, which consists of two panels.

Panel A displays the absolute annual counts of non-oncology pediatric elective surgeries, solid tumor cases, and total oncology admissions (solid tumors plus referred oncology cases) from 1996 to 2022.

Panel B presents the corresponding annual proportions of solid tumor cases and total oncology admissions relative to elective surgeries.

Across the study period, the annual number of elective surgeries remained relatively stable, ranging from a minimum of 4,613 procedures (2019) to a maximum of 5,070 procedures (2015), with only modest fluctuations, including a temporary reduction during the COVID-19 period (2019-2020). In fact, temporal stability of non-oncology pediatric elective surgical volume was evaluated using the coefficient of variation (CV) and the Mann–Kendall test for monotonic trends. Although transient reductions were observed during the COVID-19 period, formal trend testing demonstrated no significant long-term monotonic change in elective surgical volume (Mann–Kendall $\tau = 0.19$, $P = 0.17$), and overall variability remained low (CV = 2.85%). In contrast, both solid tumor case counts and total oncology admissions demonstrated a clear upward trajectory over time.

The stability of elective surgical volume, coupled with the progressive increase in oncology-related activity relative to this internal benchmark, suggests that the observed temporal patterns in pediatric oncology cases are unlikely to be driven by abrupt changes in hospital capacity, case-mix distortion, or preferential referral shifts. Rather, these findings support the internal consistency of the dataset and reinforce the validity of interpreting the results primarily in terms of temporal trends and relative distributions, rather than absolute population incidence.

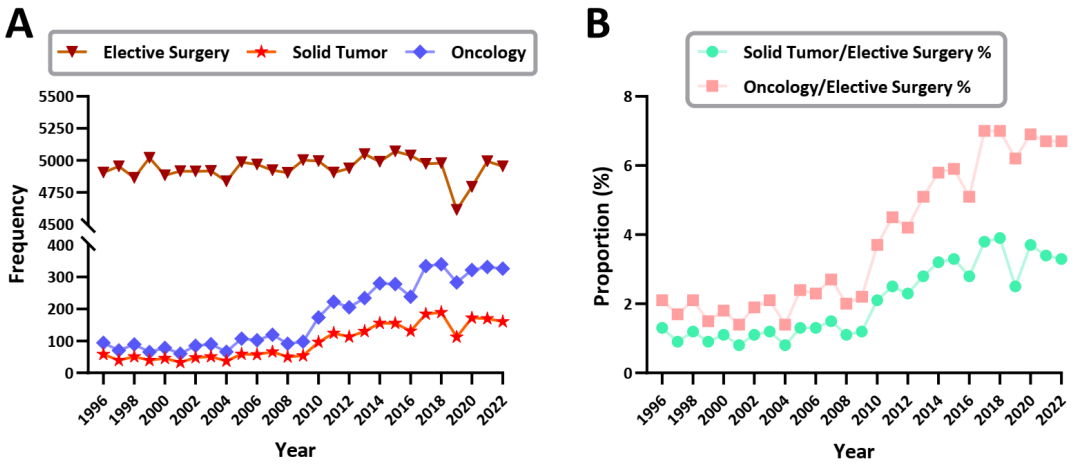

Figure S1. Internal assessment of pediatric oncology referral loads relative to non-oncology pediatric elective surgeries, 1996–2022. Panel A. Annual absolute counts of non-oncology pediatric elective surgeries (crimson inverted triangles), solid tumor cases (red stars), and total oncology admissions (blue diamonds) at the study center from 1996 to 2022. Elective surgery volume remained relatively stable over time, indicating consistent institutional capacity. Panel B. Annual proportions of solid tumor cases (green circles) and total oncology admissions (peach rectangles) relative to non-oncology pediatric elective surgeries. The stable-to-gradually increasing proportions indicate sustained and progressive oncology referral activity relative to overall surgical workload, supporting the temporal robustness of observed referral-based trends.

Supplementary Figure S2. **Exploratory Joinpoint and APC Analyses of Referral-Based Lymphomas Diagnoses by Sex and Pediatric Age Groups (1996–2022)**

Supplementary Figure S2 presents exploratory Joinpoint regression and APC analyses for referral-based Lymphomas diagnoses stratified by sex and pediatric age groups. While overall referral-based population-standardized Lymphoma rates increased steadily over the study period (AAPC = 3.52%, P < 0.001), age- and sex-specific analyses showed greater variability.

Among age groups, statistically significant upward trends were observed in children aged 1–4 years (τ = 0.410, P < 0.001) and 5–9 years (τ = 0.376, P = 0.004), whereas trends in infants (<1 year) and adolescents (10–14 years) were less stable. In infants, Joinpoint regression identified short segments with extreme APC estimates, including a sharp increase between 2014 and 2016 (APC = 119.45%, P < 0.001) followed by a decline. Given the very small number of cases contributing to these segments, interpretation relied primarily on the AAPC, which indicated an overall decrease across the full study period (AAPC = −3.47%, P = 0.040).

Sex-stratified analyses showed a stronger overall increase among females (AAPC = 4.63%) compared with males (AAPC = 2.72%), although these differences should be interpreted cautiously. Across strata, short-term fluctuations and extreme segment-specific APCs were frequently accompanied by wide confidence intervals, reflecting sparse referral counts and potential overfitting. Accordingly, these subgroup findings are presented as **exploratory and hypothesis-generating**, intended to illustrate referral-based temporal patterns rather than precise incidence changes.

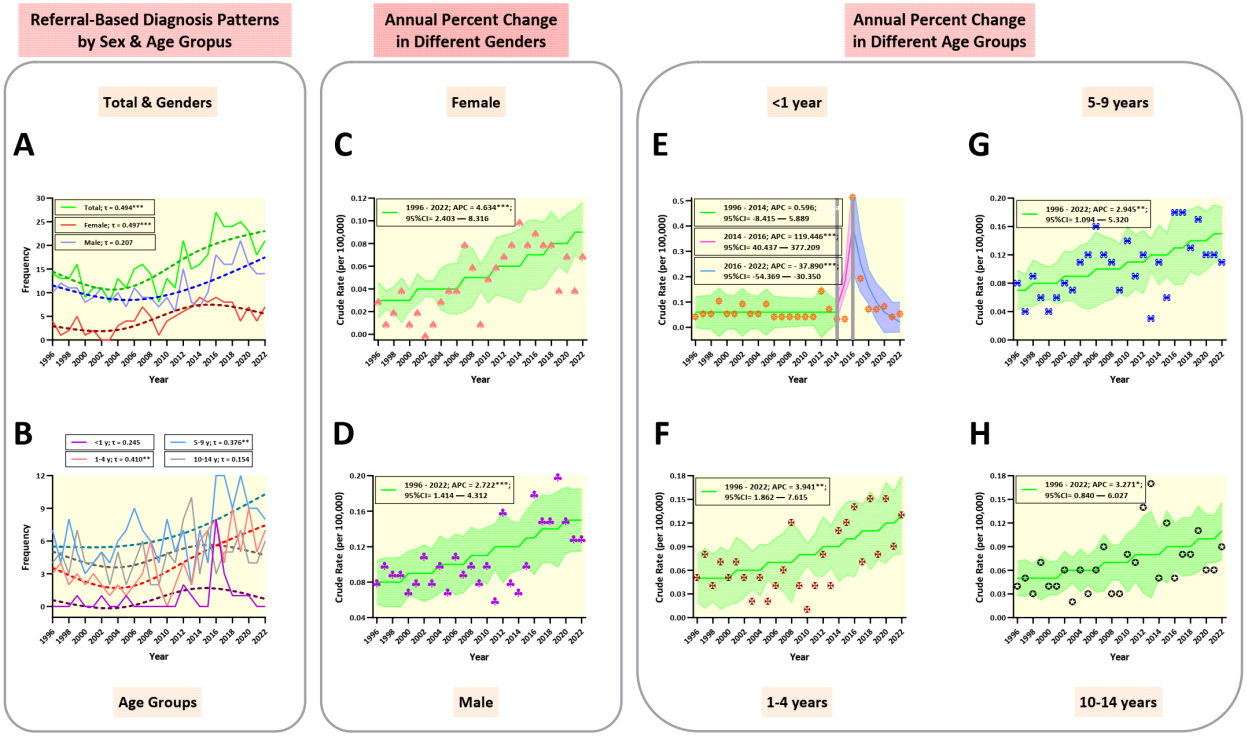

Lymphomas

Figure S2. Temporal Trends in Referral-Based Diagnosis Patterns and Annual Percent Change (APC) (based on the crude rate) of Lymphomas by Sex and Pediatric Age Groups. This figure illustrates the evolving referral-based diagnosis patterns and rate changes of Lymphomas. (**A**) Annual observed referral-based rates, presented for total

cases and disaggregated by sex. (**B**) Annual observed referral-based rates across various age groups. (**C**) APC and identified joinpoints (points where the trend significantly changes) in females. (**D**) APC and identified joinpoints in males. (**E**) APC and identified joinpoints in cases with <1 year. (**F**) APC and identified joinpoints in cases aged 1-4 years. (**G**) APC and identified joinpoints in cases aged 5-9 years. (**H**) APC and identified joinpoints in cases aged 10-14 years. Graphical Representation: Smoothed spline trend lines are shown as dashed lines. Observed crude rates are depicted by symbols. APC curves are represented by solid lines, with their standard errors indicated by the shaded areas above and below the main curve. Joinpoints are marked by vertical gray lines intersecting the x-axis. The color of the APC curves changes to indicate different trend segments: green for no joinpoint or the segment before the first, pink after the first joinpoint, and light blue after the second joinpoint. Statistical Annotations: Mann-Kendall test statistics and APC values are provided on each panel in boxes. Statistical significance is denoted by asterisks: *P<0.05, **P<0.01, and ***P<0.001. Absence of a star indicates no statistically significant difference. Rates are presented for comparative temporal analysis within this referral cohort and should not be interpreted as population-based incidence. Detailed numerical values and raw counts are provided in Table S1 [Abbreviation: APC, Annual Percent Change; CI, confidence interval; τ, Mann-Kendall trend test].

Supplementary Figure S3. **Exploratory Joinpoint and APC Analyses of Referral-Based Central Nervous System Tumor Diagnoses by Sex and Pediatric Age Groups (1996–2022).**

Supplementary Figure S3 summarizes exploratory Joinpoint regression and APC analyses for referral-based diagnoses of central nervous system (CNS) tumors stratified by sex and pediatric age groups. In contrast to Lymphomas, CNS tumors demonstrated more consistent increases across strata, although segment-specific variability remained evident.

Overall referral-based population-standardized rates increased steadily in both sexes, with a stronger rise among females (AAPC = 7.76%) compared with males (AAPC = 4.75%). Age-specific analyses showed statistically significant long-term increases across nearly all pediatric age groups, with the steepest increase observed among children aged 1–4 years (AAPC = 6.50%, P < 0.001). Adolescents aged 10–14 years showed a sustained increase beginning around 2007 (AAPC = 6.12%, P < 0.001).

Several age strata, particularly children aged 5–9 years, exhibited short Joinpoint segments with extreme APC values and wide confidence intervals, reflecting sparse referral counts within short calendar intervals. These segment-specific APCs were therefore interpreted cautiously, with greater emphasis placed on AAPCs summarizing long-term trends. As with Lymphomas, subgroup-specific findings are presented as **exploratory**, serving to highlight referral-based diagnostic patterns rather than definitive incidence changes.

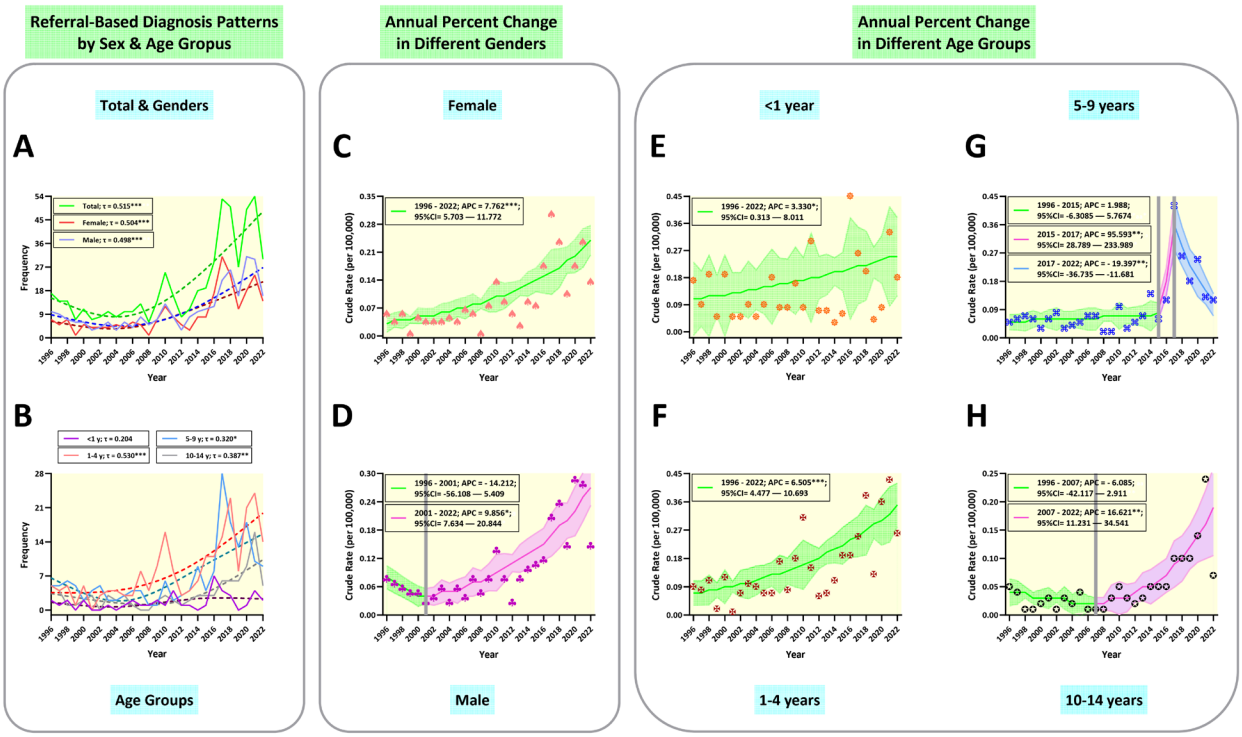

Figure S3. Temporal Trends in Referral-Based Diagnosis Patterns and Annual Percent Change (APC) (based on the crude rate) of Central Nervous System (CNS) Tumors by Sex and Pediatric Age Groups. This figure illustrates the evolving referral-based diagnosis patterns and rate changes of CNS. (**A**) Annual observed referral-based rates, presented for total cases and disaggregated by sex. (**B**) Annual observed referral-based rates across various age groups. (**C**) APC and identified joinpoints (points where the trend significantly changes) in females. (**D**) APC and identified joinpoints in males. (**E**) APC and identified joinpoints in cases with <1 year. (**F**) APC and identified joinpoints

in cases aged 1-4 years. (**G**) APC and identified joinpoints in cases aged 5-9 years. (**H**) APC and identified joinpoints in cases aged 10-14 years. Graphical Representation: Smoothed spline trend lines are shown as dashed lines. Observed crude rates are depicted by symbols. APC curves are represented by solid lines, with their standard errors indicated by the shaded areas above and below the main curve. Joinpoints are marked by vertical gray lines intersecting the x-axis. The color of the APC curves changes to indicate different trend segments: green for no joinpoint or the segment before the first, pink after the first joinpoint, and light blue after the second joinpoint. Statistical Annotations: Mann-Kendall test statistics and APC values are provided on each panel in boxes. Statistical significance is denoted by asterisks: *P<0.05, **P<0.01, and ***P<0.001. Absence of a star indicates no statistically significant difference. Rates are presented for comparative temporal analysis within this referral cohort and should not be interpreted as population-based incidence. Detailed numerical values and raw counts are provided in Table S1 [Abbreviation: APC, Annual Percent Change; CI, confidence interval; τ, Mann-Kendall trend test].

Supplementary Figure S4. **Exploratory Joinpoint and APC Analyses of Referral-Based Sympathetic Nervous System Tumor Diagnoses by Sex and Pediatric Age Groups (1996–2022).**

Supplementary Figure S4 presents exploratory Joinpoint regression and APC analyses for referral-based diagnoses of sympathetic nervous system (SNS) tumors. Among the three major tumor groups, SNS tumors demonstrated the strongest and most consistent overall increase across the study period (AAPC = 8.49%, P < 0.001).

Long-term increases were observed in both sexes, although Joinpoint analysis suggested a plateau among males after approximately 2014, reflected by a non-significant APC in the later segment. Across pediatric age groups, AAPCs ranged from 5.34% in infants to 8.22% in children aged 5–9 years (all P < 0.001), indicating sustained growth in referral-based population-standardized rates.

Despite these consistent long-term patterns, several age-specific segments showed extreme APC estimates over short intervals, accompanied by wide confidence intervals. These findings likely reflect sparse referral counts rather than abrupt changes in underlying disease occurrence. Accordingly, segment-specific APCs should be interpreted as **exploratory referral-based signals**, and emphasis should be placed on the overall AAPCs and consistency across analytical approaches.

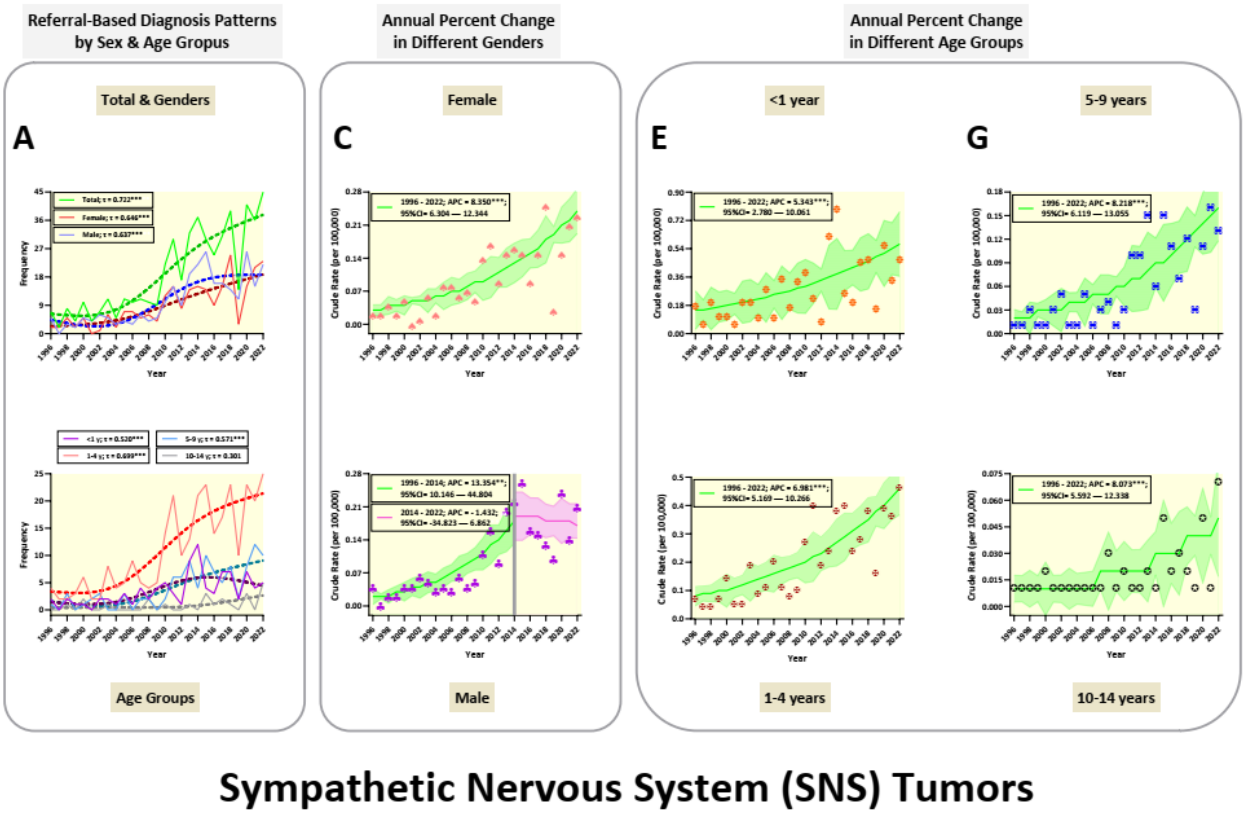

Figure S4. Temporal Trends in Referral-Based Diagnosis Patterns and Annual Percent Change (APC) (based on the crude rate) of Sympathetic Nervous System (SNS) Tumors by Sex and Pediatric Age Groups. This figure illustrates the evolving referral-based diagnosis patterns and rate changes of SNS. (**A**) Annual observed referral-based rates, presented for total cases and disaggregated by sex. (**B**) Annual observed referral-based rates across various age groups. (**C**) APC and identified joinpoints (points where the trend significantly changes) in females. (**D**) APC and identified joinpoints in males. (**E**) APC and identified joinpoints in cases with <1 year. (**F**) APC and identified joinpoints in cases aged 1-4 years. (**G**) APC and identified joinpoints in cases aged 5-9 years. (**H**) APC and identified joinpoints in cases aged 10-14 years. Graphical Representation: Smoothed spline trend lines are shown as dashed lines. Observed

crude rates are depicted by symbols. APC curves are represented by solid lines, with their standard errors indicated by the shaded areas above and below the main curve. Joinpoints are marked by vertical gray lines intersecting the x-axis. The color of the APC curves changes to indicate different trend segments: green for no joinpoint or the segment before the first, pink after the first joinpoint, and light blue after the second joinpoint. Statistical Annotations: Mann-Kendall test statistics and APC values are provided on each panel in boxes. Statistical significance is denoted by asterisks: *P<0.05, **P<0.01, and ***P<0.001. Absence of a star indicates no statistically significant difference. Rates are presented for comparative temporal analysis within this referral cohort and should not be interpreted as population-based incidence. Detailed numerical values and raw counts are provided in Table S1 [Abbreviation: APC, Annual Percent Change; CI, confidence interval; τ, Mann-Kendall trend test].

Supplementary Figure S5. **Age- and cohort-specific predicted referral-based diagnosis rates for pediatric solid tumors (1996–2022).**

Across tumor types, age-specific referral-based diagnosis patterns differed substantially, reflecting strong tumor-specific age dependencies (Figure S5A–C). Central nervous system (CNS) and sympathetic nervous system (SNS) tumors showed their highest predicted diagnosis rates in the youngest age group (0–4 years), followed by marked declines in older pediatric age groups. These patterns were supported by statistically significant linear and higher-order age terms in the Age–Period–Cohort models, indicating pronounced and non-linear age-related variation in referral-based diagnosis patterns (Tables S4 and S5). In contrast, Lymphomas demonstrated a comparatively flatter age profile, with more uniform predicted diagnosis rates across pediatric age groups and weaker age gradients overall (Figure S5A; Table S3).

Cohort-specific predicted referral-based diagnosis rates, displayed jointly for all tumor types (Figure S5D), showed heterogeneous and non-monotonic patterns. CNS tumors exhibited higher predicted diagnosis rates in several more recent birth cohorts, broadly consistent with the strong calendar period effects observed in the main analysis. Lymphomas displayed variable cohort-related fluctuations without a consistent monotonic pattern, while SNS cohort estimates were comparatively unstable, characterized by wide confidence intervals and limited statistical precision, reflecting sparse data and inherent identifiability constraints of Age–Period–Cohort models. Accordingly, cohort-specific outputs are presented as descriptive, smoothed temporal components rather than cohort-specific incidence or risk estimates (Tables S3–S5).

All age- and cohort-specific estimates shown in Figure S5 are model-based predictions derived from quasi-Poisson Age–Period–Cohort models and should be interpreted as summaries of underlying temporal structure rather than exact cell-specific rates. These results are provided to complement the period-focused findings in the main text and to illustrate the broader age and cohort patterns underlying observed referral-based temporal trends.

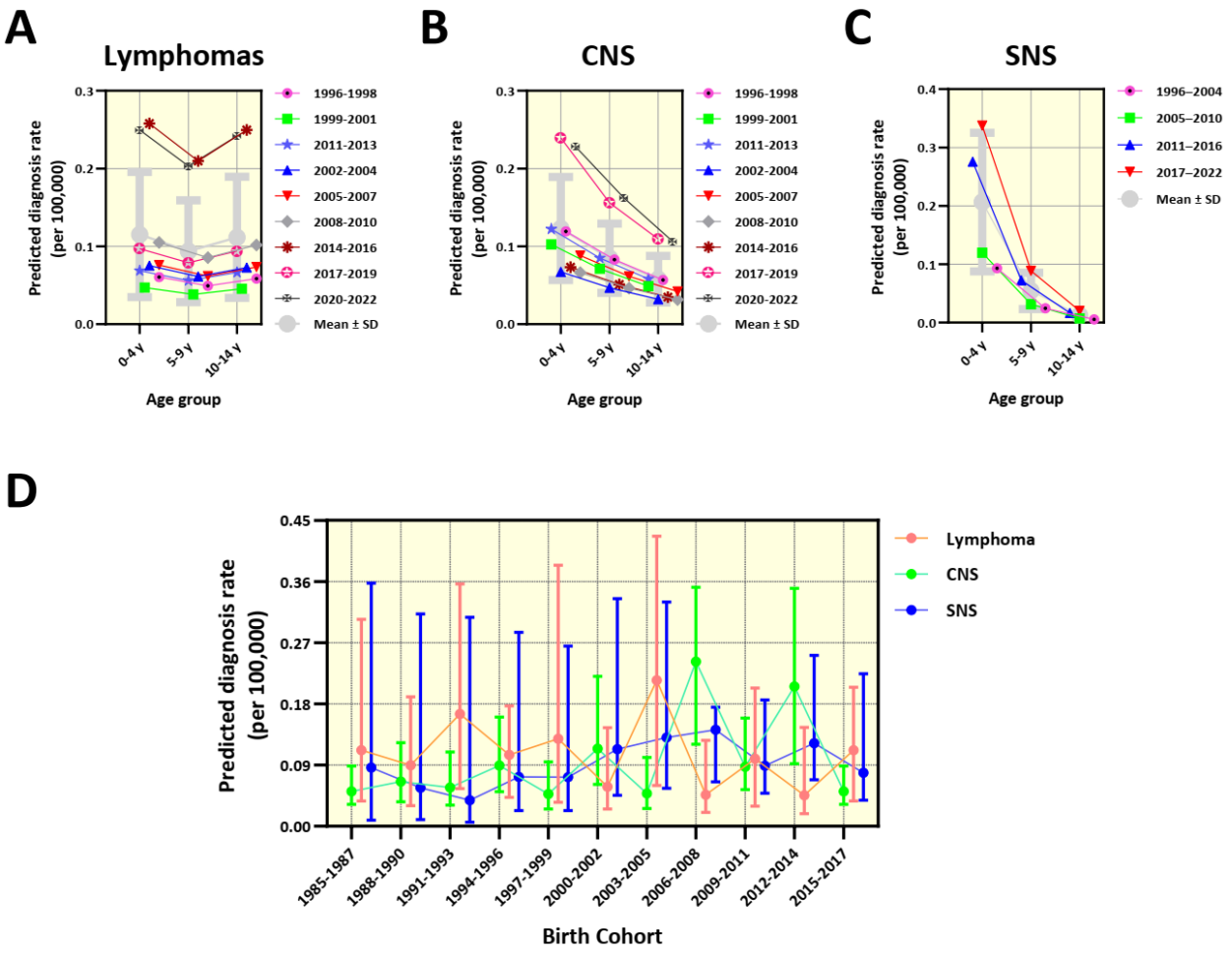

Figure S5. Age- and cohort-specific predicted referral-based diagnosis rates for pediatric solid tumors (1996–2022). (**A**) Mean predicted age-specific referral-based rates for Lymphomas. (**B**) Mean predicted age-specific referral-based rates for central nervous system (CNS) tumors. (**C**) Mean predicted age-specific referral-based rates for sympathetic nervous system (SNS) tumors. (**D**) mean predicted cohort-specific referral-based rates for Lymphomas, CNS, and SNS tumors. All rates are expressed per 100,000 population. Error bars in panels A–C represent standard deviations (SDs) around mean age-specific predicted rates, whereas error bars in panel D indicate 95% confidence intervals derived from quasi-Poisson Age–Period–Cohort models. Estimates reflect smoothed age and cohort components of the Age–Period–Cohort models and should not be interpreted as cohort-specific incidence or risk. For visualization clarity, some symbols were slightly offset along the x-axis [Abbreviation: CNS, Central Nervous System; SNS, Sympathetic Nervous System; y, year(s)].